Proc. Natl. Acad. Sci. USA
Vol. 83, pp. 1675–1679, March 1986
Biochemistry

Expression of a cDNA derived from the yeast killer preprotoxin gene: Implications for processing and immunity

(*Saccharomyces cerevisiae*/toxin/secretion/acid phosphatase/double-stranded RNA)

STEVEN D. HANES*, VIRGINIA E. BURN*, STEPHEN L. STURLEY*, DONALD J. TIPPER†, AND KEITH A. BOSTIAN*

*Section of Biochemistry, Division of Biology and Medicine, Brown University, Providence, RI 02912; and †Department of Molecular Genetics and Microbiology, University of Massachusetts Medical School, Worcester, MA 01606

Communicated by W. K. Joklik, November 14, 1985

ABSTRACT **The type I killer strains of *Saccharomyces cerevisiae* secrete a dimeric 19-kDa protein that kills sensitive cells by disrupting cytoplasmic membrane function. This toxin is encoded by the double-stranded RNA plasmid M_1-dsRNA, which also determines specific immunity to toxin. A preprotoxin, the 35-kDa *in vitro* translation product of denatured M_1-dsRNA, is presumed to be the primary *in vivo* gene product. To facilitate studies on preprotoxin structure and maturation, we have inserted a partial cDNA copy of M_1-dsRNA into the yeast vector p1A1, bringing it under control of the phosphate-repressible *PHO5* promoter. This in-frame gene fusion encodes all of the preprotoxin sequence except for its N-terminal secretion leader, which is replaced by the leader sequence of *PHO5*. Transformation of sensitive yeast strains lacking M_1-dsRNA with such fusion plasmids converts them to phosphate-repressible, immune killers, demonstrating that both toxin and immunity determinants are contained within the preprotoxin molecule. L-1-Tosylamido-2-phenylethyl chloromethyl ketone retards glycosylation of preprotoxin to toxin, facilitating size comparisons and indicating that processing of the normal precursor involves three glycosylation events but does not involve cotranslational leader peptidase action. In contrast, the *PHO5* leader is apparently removed from the fusion preprotoxin.**

The determinant of toxin production and of specific immunity to this toxin in the type I killer system of *Saccharomyces cerevisiae* (1, 2) is the 1.9-kilobase-pair (kb) double-stranded RNA plasmid M_1-dsRNA, which is encapsidated in cytoplasmic virus-like particles, ScV-M_1. The secreted toxin is encoded by M_1-dsRNA (3) and is composed of two dissimilar, 9.5- and 9.0-kDa, disulfide-linked, nonglycosylated protein subunits, denoted α and β, respectively (4). An intracellular 43-kDa glycosylated precursor, or protoxin, is precipitated from extracts of pulse-labeled killer cells by anti-toxin IgG (5, 6) and is processed, with a half-life of about 25 min, into the 19-kDa exocellular toxin (7). *In vitro* translation of denatured M_1-dsRNA produces M_1-P1, a 35-kDa product (3, 4).

Comparison of the N-terminal sequences of the α and β toxin subunits with the nucleotide sequence of a cDNA clone, derived from an *in vivo* M_1-dsRNA transcript (8), has enabled us to localize the coding domains for these toxin subunits within the M_1 genome (4). Both are contained within a 316-codon open reading frame, initiating 14 base pairs (bp) from the 5′ terminus of the plus strand of M_1-dsRNA (9), that encodes a 34.8-kDa product. This is believed to be identical to M_1-P1, which has the predicted N-terminal sequence, and to be the *in vivo* primary translation product, or preprotoxin (4). The α toxin component in preprotoxin is preceded by a 44 amino acid N-terminal segment called δ (4) (see Fig. 1*C*). This segment has a typical hydrophobic leader peptide sequence (10) between residues 7 and 27. Following α is a segment called γ, estimated to be 103 amino acids long (its startpoint is not precisely known), with the β toxin component comprising the C-terminal segment of preprotoxin. γ contains all three of the potential asparagine-glycosylation sites and is hypothesized to be the immunity determinant (3, 4, 6).

To confirm and extend these findings, we have inserted a cDNA copy of the preprotoxin gene into the yeast shuttle vector p1A1, placing it under control of the repressible yeast acid phosphatase *PHO5* promoter (11). This hybrid gene displays phosphate-repressible expression of both killer and immunity phenotypes.

MATERIALS AND METHODS

Yeast Strains, Media, and Toxin Assays. Strains S6 (a/α) and GG100-14D (α *his3 ura3 trp1 pho5 pho3*) lack M_1-dsRNA and are sensitive to toxin. Strain K12-1 (α *ade arg*) contains M_1-dsRNA and is the standard type K1 killer used in previous studies (3, 4, 6, 8). The diploid strain T158C/S14a has also been described previously (7). Low-phosphate (low-P_i) and high-phosphate (high-P_i) media (12, 13) were employed for growth of yeast strains under repressed (high-P_i) or derepressed (low-P_i) conditions for *PHO5* and were used in standard patch assays (14) for toxin and immunity.

Construction of pSH-GB Expression Plasmids and Yeast Transformation. The 1030-bp *Ava* II–*Pst* I fragment of pH4G1 DNA (4), containing the preprotoxin sequence, was made blunt-ended by treatment with the Klenow fragment of DNA polymerase I and ligated to *Bam*HI linkers (New England Biolabs, 5′ CGCGGATCCGCG 3′). After *Bam*HI digestion, the fragment was inserted into the *Bam*HI site of pBR322. Transformants of *Escherichia coli* strain MC1061 were identified by colony hybridization (15) with radiolabeled single-stranded probe prepared from a recombinant M13 mp8 phage containing a 372-bp (*Hin*fI–*Bgl* I) region of the preprotoxin cDNA (8). The *Bam*HI fragment from one such clone, pSH-C60, was Klenow-treated and ligated to linearized vector 1A1 (previously *Kpn* I digested and treated with Klenow fragment). Transformants of *E. coli* MC1061 cells were identified with the probe described above, and restriction digests of plasmid minipreparations were analyzed to determine the orientation of the inserted preprotoxin sequence. Cells of yeast strain GG100-14D were transformed (11) with several of the pSH-GB recombinant plasmids. Ura^+ clones were analyzed for killer phenotype.

Isolation and *in Vitro* Translation of Total Cellular RNAs. Total RNA was isolated from cells grown in low-P_i or high-P_i

The publication costs of this article were defrayed in part by page charge payment. This article must therefore be hereby marked "*advertisement*" in accordance with 18 U.S.C. §1734 solely to indicate this fact.

Abbreviations: bp, base pair(s); kb, kilobase pair(s); TPCK, L-1-tosylamido-2-phenylethyl chloromethyl ketone.

medium, as described (6, 8). Undenatured RNAs were translated in a wheat germ system, with L-[^{35}S]methionine, and the radiolabeled translation products were analyzed by immunoprecipitation with a mixture of anti-toxin (3) and anti-enolase IgGs, fractionation by NaDodSO$_4$/10% PAGE, and autoradiography, as described (3, 4, 13).

Labeling and Immunoprecipitation of *in Vivo* Protoxin. Cells, grown on low-P$_i$ or high-P$_i$ medium to a density of 2.5 $\times$ 10^7 cells per ml, were pulse-labeled with L-[^{35}S]methionine for 12 min prior to preparation of cell extracts in the presence of Triton X-100, as described (6). The products were analyzed by immunoprecipitation and gel electrophoresis as described above. The specificity of immunoprecipitation was demonstrated by the selectivity of the competitive effects of addition of increasing quantities (0.2–0.6 μg) of purified killer toxin. Where indicated, cells were pretreated with 5 mM L-1-tosylamido-2-phenylethyl chloromethyl ketone (TPCK) for 10 min at 30°C before pulse-labeling. In pulse–chase experiments, incubation was continued for various periods in the presence of 3 mM L-methionine prior to harvesting as described (7). Where indicated, extracts were digested with endoglycosidase H (6) prior to immunoprecipitation.

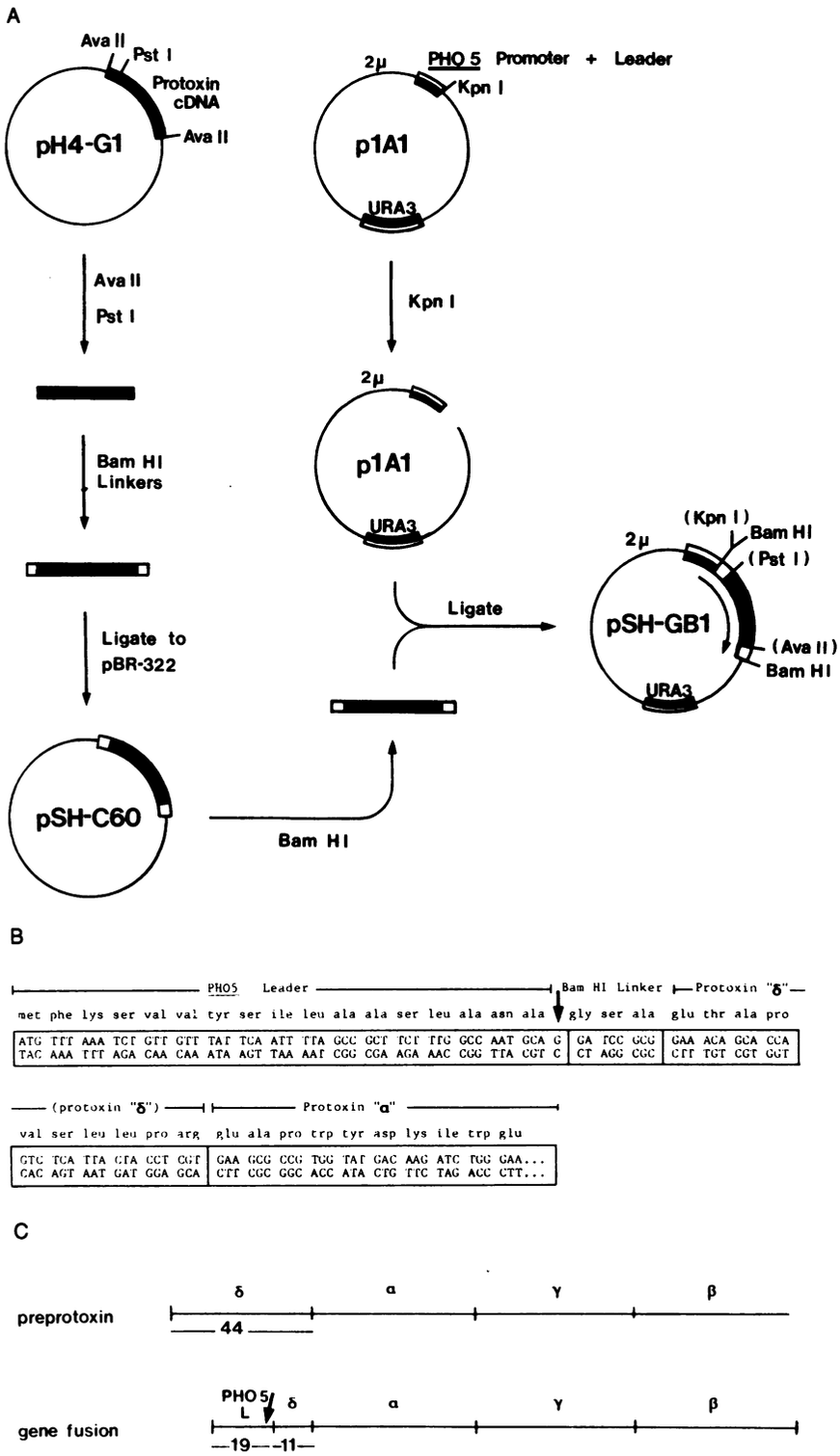

FIG. 1. Fusion of preprotoxin cDNA to the *PHO5* promoter. (*A*) Construction of plasmids for expression of protoxin in yeast. pSH-GB1 was constructed by attachment of *Bam*HI linkers to the *Pst* I–*Ava* II fragment of the M$_1$-cDNA clone pH4G1 (8), which was then inserted into the *Bam*HI site of pBR322. This insert was then removed by digestion with *Bam*HI and blunt-end-ligated into the *Kpn* I site of the yeast shuttle vector p1A1. This vector is a restriction-site-modified form of the plasmid YEp24, containing the *Bam*HI–*Sal* I *PHO5* promoter fragment (12, 13). This construction creates a fusion of the protoxin δ domain to the leader sequence of acid phosphatase. (2 μ, Sequences from the yeast 2-μm plasmid conferring autonomous replication.) (*B*) Proposed DNA sequence in the fusion region of the pSH-GB series of preprotoxin expression plasmids. The gene fusion joins the 17 amino acid leader peptide sequence of acid phosphatase (12, 13) (under control of the *PHO5* promoter) to the *Pst* I site of the protoxin. The *Bam*HI linker serves to align the fusion in-frame and recreates the Ala-Gly cleavage site of the phosphatase leader peptide. The third residue encoded by the *Bam*HI linker (Ala) is equivalent to residue 34 of the wild-type preprotoxin molecule. (*C*) Functional domains of the normal preprotoxin and of the fusion gene products. Numbers refer to amino acid residues in the N-terminal segment preceding the α-toxin component. *PHO5* L includes the 17 amino acid acid phosphatase leader, with the putative cleavage site (arrow), plus 2 residues encoded by the *Bam*HI linker.

RESULTS AND DISCUSSION

Construction of the *PHO5*-M_1 cDNA Gene Fusion and Expression in Yeast. Details for the construction of the *PHO5*-M_1 cDNA fusion are shown in Fig. 1. The *Pst* I–*Ava* II fragment of pH4G1 includes an 895-bp segment of M_1 cDNA (4), starting 111 bp from the 5′ terminus of the plus strand of M_1-dsRNA, joined by a $d(G{\cdot}C)_n$ tail to a short fragment of pBR322. It contains the entire preprotoxin gene except for the presumed translation start site and the first 32 amino acids of the δ segment (Fig. 1*A*). *Bam*HI linkers were used to fuse this, in-frame, to a 5′ portion of the acid phosphatase *PHO5* gene (12) that included the promoter, the translation start site, and the 17 amino acid acid phosphatase leader-peptide sequence (Fig. 1*B*). The resulting hybrid gene contained the normal acid phosphatase Ala-Gly leader peptidase cleavage site at residues 17–18 and, from residue 20 onwards, the normal sequence of preprotoxin from residue 34 (Fig. 1 *B* and *C*). This fusion junction was confirmed by DNA sequence analysis of plasmid pSH-GB16. The pSH-GB plasmids containing this hybrid gene, independently isolated from a single *E. coli* transformation, were used to transform non-killer yeast (GG100-14D). Both killing and immunity phenotypes were expressed in a manner consistent with the known properties of the *PHO5* promoter (Fig. 2) (11, 13). Under derepressed conditions (low-P_i medium), levels of toxin production and immunity approximated those seen in the standard killer strain K12-1 (Fig. 2).

Preprotoxin Contains a Component Determining Toxin Immunity. Mutations in M_1-dsRNA are known that lead to loss of either immunity or killer properties (2, 5), and it has been hypothesized (4, 6) that the glycosylated γ segment of protoxin (Fig. 1*C*) is the immunity determinant. Although one could not previously rule out the existence of an independent M_1-dsRNA gene product responsible for immunity, the present data show that both the killer and immunity phenotypes are encoded in the same transcriptional unit, with one open reading frame, in this case under control of a single (*PHO5*) promoter. This implies that the immunity component resides within the preprotoxin molecule, presumably in the γ domain. Analysis of an almost identical M_1 cDNA, expressed in yeast and under the control of the *ADH1* promoter, has led to similar conclusions (16). A role for δ, the other nontoxin component of preprotoxin, in immunity seems unlikely, since most of it is missing in the fusion gene product.

Analysis of *in Vivo* Transcripts of *PHO5*-M_1 cDNA Gene Fusions. Yeast transformants, named according to the particular pSH-GB plasmid that they contain (e.g., yGB-16 was transformed with pSH-GB16), were further analyzed by *in vitro* translation of RNA isolated from repressed or derepressed cells and precipitation with anti-toxin. The major translation product derived from M_1-dsRNA transcripts from the standard killer strain K12-1 is identical to M_1-P1, a 35-kDa species (ref. 8; Fig. 3*A*, lanes b and d). The crossreactive fusion gene translation product, M_1-$P1_{hy}$, derived from transformant cell transcripts, migrated as a 33-kDa species (Fig. 3*A*, lane f), consistent with the 14 amino acid reduction in size of its N-terminal sequence (Fig. 1*C*). M_1-$P1_{hy}$ was detected in translation products of RNA extracted from transformant cells grown in low-P_i medium but not of RNA from cells grown in high-P_i medium (Fig. 3*A*, lanes f and h). The doublet of proteins appearing at about 50 kDa was precipitated by anti-enolase IgG, included as an internal standard for the mRNA assay. Translation products of RNAs from several other transformants with a phosphate-repressible killer phenotype (yGB-1, -2, -5, -7, -8, and -15, Fig. 2) contained an M_1-$P1_{hy}$ species of identical size (results not shown).

The regulated expression of the hybrid RNA transcripts and their relative cellular concentrations were also confirmed by blot hybridization analysis of electrophoretically fractionated cellular RNA, using a preprotoxin cDNA probe (data not shown). Transcripts of about 1.0 kb were detected in derepressed cells and their concentration was approximately

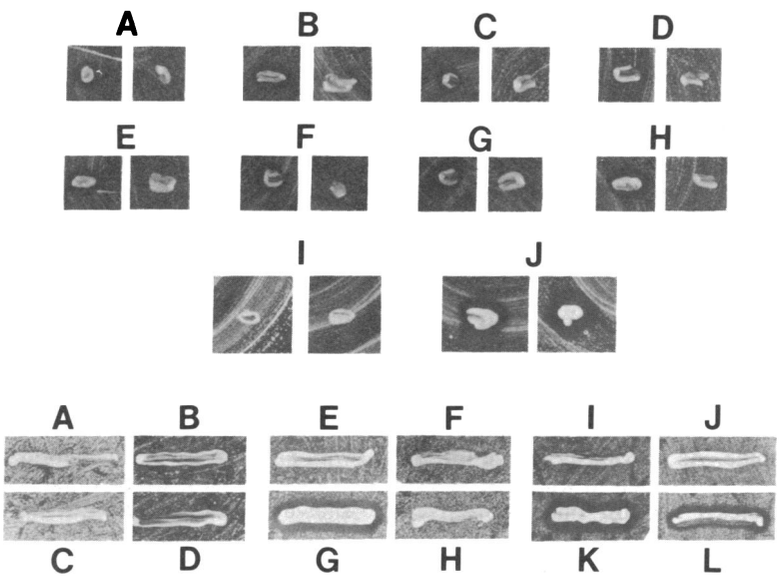

FIG. 2. Killer and immunity phenotype of M_1-cDNA transformants grown under repressed or derepressed conditions. (*Upper*) Each pair (*A–J*) shows an individual transformant assayed for the production of type 1 killer toxin by a standard plate patch assay (14) on low-P_i medium (derepressed, left) or high-P_i medium (repressed, right). A lawn of 10^6 cells of sensitive strain S6 was applied to each plate (*A–J*) and tester strains (transformants), previously grown in low-P_i or high-P_i liquid medium, were "patched," respectively, onto low-P_i or high-P_i plates and analyzed after 48 hr for zones of growth inhibition. Cells patched were yGB-1 (*A*), yGB-2 (*B*), yGB-5 (*C*), yGB-6 (*D*), yGB-7 (*E*), yGB-8 (*F*), yGB-15 (*G*), and yGB-16 (*H*). Controls were sensitive recipient GG100-14D (*I*) and wild-type killer K12-1 (*J*). (*Lower*) The transformant strain yGB-16 (*E–H*), control killer K12-1 (*A–D*), and sensitive strain S6 (*I–L*) were assayed for immunity to K12-1 toxin by a reciprocal assay to the toxin-production assay described above. Lawns of transformant and control strains were prepared from cells grown in low-P_i or high-P_i medium and plated onto low-P_i- or high-P_i-medium plates (right and left pair in each group, respectively). These were patched with cells of the sensitive strain S6 (upper row) or the killer strain K12-1 (lower row), and analyzed after 48 hr for the absence of zones of growth inhibition (immunity).

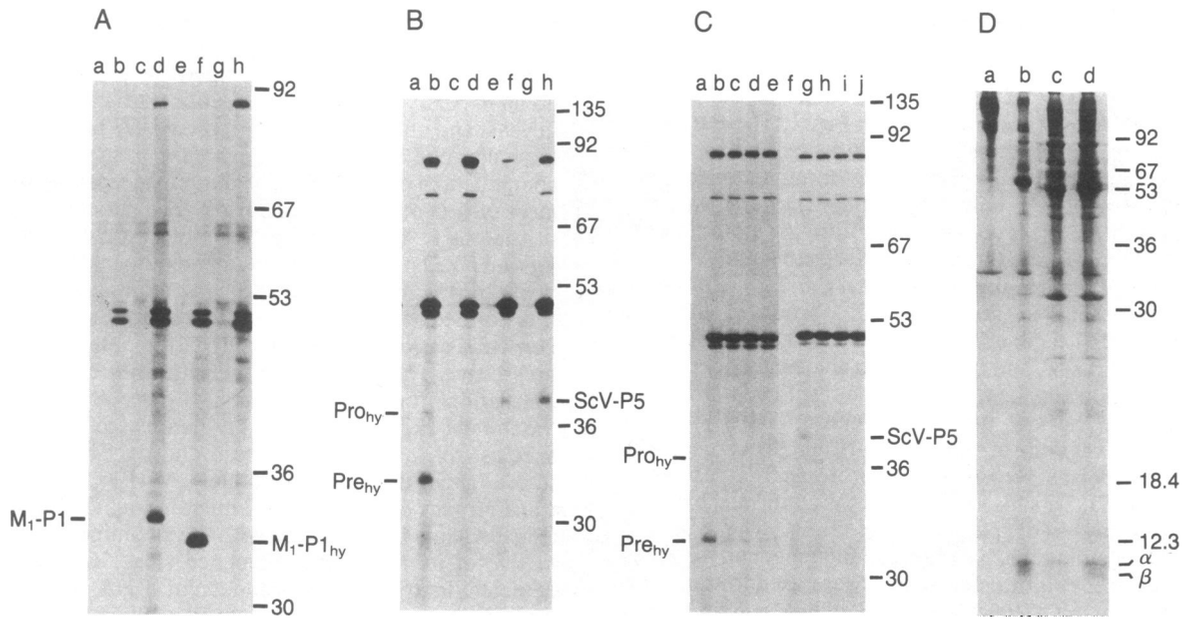

FIG. 3. Composite gel autoradiograms of *in vitro*- and *in vivo*-derived [^{35}S]methionine-labeled protein from M_1 cDNA transformants. (*A*) Total RNA was prepared from wild-type killer strain K12-1 (lanes a–d) and transformant yGB-16 (lanes e–h). Cells were grown in either high-P_i medium (lanes c, d, g, and h) or low-P_i medium (lanes a, b, e, and f). Undenatured RNA was translated and the products were analyzed by immunoprecipitation with a mixture of anti-toxin and anti-enolase IgGs as described in the text. Controls (lanes a, c, e, and g) were incubated with preimmune serum in place of immune IgGs. Since enolase is a major constitutive enzyme, the two enolase bands at about 50 kDa act as internal controls for the efficiency of mRNA recovery, translation, and immunoprecipitation. The positions of 34.8-kDa preprotoxin (M_1-P1) and the 33-kDa product from the transcript of the fused gene (M_1-$P1_{hy}$) are indicated. (*B*) Extracts of pulse-labeled cells of wild-type killer K12-1 (lanes e–h) and transformant yGB-16 (lanes a–d) grown in high-P_i medium (lanes c, d, g, and h) or low-P_i medium (lanes a, b, e, and f) were immunoprecipitated and analyzed as in *A* with a mixture of anti-toxin and anti-enolase IgGs (lanes b, d, f, and h) or with preimmune IgG (lanes a, c, e, and g). ScV-P5 is the 43-kDa glycosylated protoxin produced in wild-type killer cells (6). Pro_{hy} (lane b) is presumably the equivalent glycosylated precursor formed in the transformants. Pre_{hy} (lane b), a 33-kDa protein, is presumably equivalent to the M_1-$P1_{hy}$ synthesized *in vitro* (see *A*), with which it comigrates on NaDodSO$_4$ polyacrylamide gels (data not shown). (*C*) The specificity of immunoprecipitation of the Pre_{hy} species was determined by immunocompetition assay with native exocellular toxin. Lanes f and g are equivalent to lanes e and f in *B*, showing *in vivo*-labeled wild-type protoxin (ScV-P5). Lanes h–j are identical to lane g, except that immunoprecipitation was performed in the presence of 0.2, 0.4, and 0.6 μg of killer toxin, respectively. Lanes a and b are equivalent to lanes a and b in *A*, showing *in vivo*-labeled hybrid protoxin (Pro_{hy}) and preprotoxin (Pre_{hy}). Lanes c–e are equivalent to lane b, except for immunocompetition, as in lanes g–j. (*D*) The toxin components, α and β, were detected among the total secreted proteins of the transformant strain yGB-16 by NaDodSO$_4$/PAGE in the presence of 2-mercaptoethanol, followed by staining with Coomassie blue (4). Cells of the transformant strain yGB-16 were grown in high-P_i (lane a) or low-P_i (lane b) medium, and the cell-free media were concentrated by ultrafiltration through an Amicon PM10 membrane (5). For comparison, cells of the toxin-producing strain K12-1, grown in low-P_i medium, were analyzed separately (lane c) or mixed with an equal amount of the low-P_i-grown transformant yGB-16 cells (lane d). In *A–D*, positions and sizes (in kDa) of markers run in the same gel are indicated.

proportional to the *in vitro* translational activity of M_1-$P1_{hy}$ mRNA, suggesting that these chimeric plasmid-encoded transcripts are efficiently processed and transported out of the nucleus in the absence of any known transcriptional-termination or poly(A)-addition sites. The 3′ end of the protoxin cDNA includes a poly(G) tract ≈20 bp long, which may play a role in transcriptional termination.

Detection of Intracellular Protoxin and Secreted Toxin in yGB Transformants. The *in vivo* products of the *PHO5* preprotoxin hybrid fusion genes were analyzed by immunoprecipitation of extracts of transformed cells metabolically labeled with L-[^{35}S]methionine. As previously shown (6), a 43-kDa intracellular protoxin is detected in wild-type killer cells (ScV-P5; Fig. 3*B*, lanes f and h). Immunoreactive species were detected in transformed cells grown in low-P_i medium (Fig. 3*B*, lane b), but not in high-P_i medium (Fig. 3*B*, lane d). These species, with apparent molecular masses of 33 and 40 kDa, are presumed to represent the hybrid gene preprotoxin and glycosylated hybrid protoxin, respectively. Addition of increasing quantities of wild-type toxin competed for immunoprecipitation of both species, confirming the specificity of the immunoprecipitation (Fig. 3*C*, lanes b–e). Competition for immunoprecipitation of ScV-P5, the normal 43-kDa protoxin, was similar (Fig. 3*C*, lanes g–j). Proteins secreted from cells of yGB-16 transformants and from control K12-1 cells were concentrated and examined for the presence of the toxin components α and β by NaDodSO$_4$/PAGE (Fig. 3*D*). Derepressed yGB-16 transformant cells (Fig. 3*D*, lane b) produced apparently normal α and β polypeptides in the same proportion as wild-type cells (Fig. 3*D*, lane c) and at somewhat higher levels.

The phosphate-repressible killer and immunity phenotypes expressed by the pSH-GB transformants demonstrate that the sequence of M_1-P1 preprotoxin, derived from the cDNA sequence (4), corresponds to the functional gene. Secretion and processing apparently occur with only moderate efficiency, judged by the observed levels of hybrid preprotoxin, but with high fidelity in this hybrid molecule.

TPCK Retards Glycosylation of Protoxin. It was previously shown (7) that in cells pretreated with TPCK, an inhibitor of chymotrypsin-like serine proteases, accumulation of labeled protoxin occurred during a 40-min chase. Inhibition of cleavage at a chymotrypsin-type site between α and γ was proposed as an explanation (4). Immediately following exposure of labeled cells to TPCK, however, antitoxin IgG precipitates four species from extracts of the cells, the largest with the mobility of protoxin and the smallest with the mobility of M_1-P1 (Fig. 4, lane d). Following a chase, only protoxin is seen, as before (Fig. 4, lanes k and l). The mobility difference between each band approximates that expected for a $(GlcNAc)_2(Gal)_9$-core glycosyl unit. The simplest interpretation is that TPCK retards glycosylation of M_1-P1 so that the

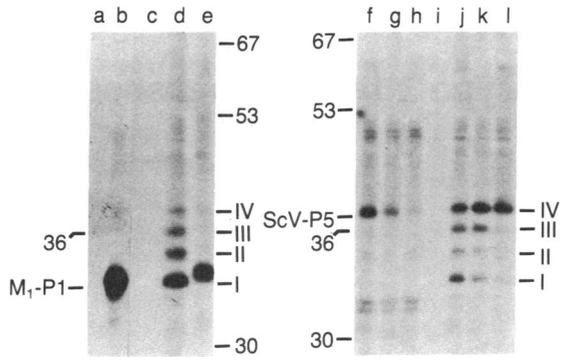

FIG. 4. Accumulation of partially glycosylated protoxin in the presence of TPCK. Lanes a and b: *in vitro* translation products of denatured M_1-dsRNA, immunoprecipitated with preimmune serum or anti-toxin IgG, respectively. Lanes c and d: protein from pulse-labeled cell extracts of strain T158C/S14a treated with TPCK as described in the text, immunoprecipitated with preimmune serum or anti-toxin IgG, respectively. Species I, from TPCK-treated cells, comigrates with the major product of *in vitro* translation of M_1-dsRNA, M_1-P1 (lane b); and species IV has the same mobility as wild-type protoxin, ScV-P5. These proteins and intermediates (II and III) differ only in the relative degree of glycosylation, as shown by endoglycosidase H treatment of a portion of the sample used for lane d (lane e). Lanes f–h: protein immunoprecipitated (with anti-toxin IgG) from pulse-labeled-cell extracts of the same strain, after unlabeled-methionine chases of 2.5, 10, and 40 min, respectively. Lanes j–l: same as lanes f–h except that cells were treated with TPCK. Lane i: control similar to lane j except that preimmune serum was used.

four bands correspond to M_1-P1 carrying 0, 1, 2, and the maximum of 3 glycosyl units. Endoglycosidase H converts all species to a product slightly larger than M_1-P1 (Fig. 4, lane e), consistent with the retention of single GlcNAc residues.

An analogous pattern of four partial glycosylation products is seen for the prepro α-factor gene MFα1 when overexpressed in *sec59* cells at the nonpermissive temperature (17). Although the site of action of TPCK in the secretion pathway of yeast is unknown, the phenotype suggests an early block during entry into the endoplasmic reticulum, as proposed for *sec59* (17). However, it is also possible that blockage of a later event leads to feedback accumulation of early intermediates. Multiple sensitive steps may exist, including the originally proposed γ-cleavage event. However, since TPCK also retards glycosylation of acid phosphatase (unpublished observations), such inhibition cannot be responsible for nonspecific delayed glycosylation.

The nonglycosylated preprotoxin produced in cells treated with tunicamycin has a gel mobility identical to that of M_1-P1 (7), slightly faster than the product of treatment of protoxin with endoglycosidase H (6). As deduced from similar data for the α-factor precursor (17), retention of the leader peptide during entry of preprotoxin into the endoplasmic reticulum is indicated. The mobilities of the "ladder" of products seen in the presence of TPCK provide strong support for this conclusion, as do the mobilities of the *PHO5*-M_1 cDNA fusion gene products. The glycosylated hybrid protoxin (40 kDa) is 3 kDa smaller than ScV-P5 (43 kDa), corresponding to the 31 amino acid difference expected if processing removes only the *PHO5* leader peptide of the hybrid preprotoxin. Since this size difference persists after endoglycosidase H digestion of ScV-P5 and the hybrid protoxin (results not shown), both molecules are glycosylated to equal extents.

Clear parallels exist between the functional organization of the yeast mating-factor precursor (17, 18) and that of the preprotoxin gene. Both have a typical N-terminal leader, a large central region containing three potential glycosylation sites, and a C-terminal region that becomes a secreted nonglycosylated fragment. In both cases, the secreted products result from cleavage events occurring late in the secretion pathway, including cleavage by the *KEX2* Lys-Arg endopeptidase (19, 20). This may obviate requirements for leader-peptide removal. Alternatively, efficient maturation of this type of gene product in yeast may require anchoring of the precursor to the membranes of the secretory pathway as a consequence of retention of the leader sequence. Such unique events may include avoidance of additional glycosylation in the Golgi apparatus; functions of the *KEX1*, *KEX2*, and *STE13* gene products (19); and TPCK-sensitive endopeptidase cleavage in secretion vesicles (7). However, since toxin and immunity are expressed by the *PHO5* fusion gene, leader-peptide retention is clearly not essential, although the levels of toxin secreted are far less than anticipated for the derepressed *PHO5* promoter.

The predominant 33-kDa intracellular species seen in derepressed, pulse-labeled yGB-16 cells (Fig. 3) is presumed to be unprocessed hybrid preprotoxin. This may reflect inefficiency of insertion of the hybrid molecule into the endoplasmic reticulum because of hybrid domains in the leader region, overloading of the secretion pathway, or, possibly, downstream problems associated with removal of the *PHO5* leader. The intracellular location of this aberrant product is unknown but is most likely cytoplasmic. As anticipated, the derepressed *PHO5* promoter expresses hybrid preprotoxin mRNA at much higher levels than the native ScV-M_1 plasmid. Diversion of most of the product may protect the cells from suicidal levels of toxin production.

This work was supported in part by National Institutes of Health Biomedical Research Support Grant RR05644-15 (K.A.B.), by a grant from Biotechnology General, Inc. (K.A.B.), and by Department of Health and Human Services Grant GM20755 (D.J.T.).

1. Bevan, E. A., Herring, A. J. & Mitchell, D. J. (1973) *Nature (London)* **245**, 81–86.
2. Bussey, H. (1981) in *Advances in Microbial Physiology*, eds. Rose, A. H. & Morris, G. (Academic, New York), Vol. 22, pp. 93–112.
3. Bostian, K. A., Hopper, J. E., Rogers, D. T. & Tipper, D. J. (1980) *Cell* **19**, 403–414.
4. Bostian, K., Elliot, Q., Bussey, H., Burn, V., Smith, A. & Tipper, D. J. (1984) *Cell* **36**, 741–751.
5. Bussey, H., Sacks, W., Galley, D. & Saville, D. (1982) *Mol. Cell. Biol.* **2**, 346–354.
6. Bostian, K. A., Jayachandran, S. & Tipper, D. J. (1983) *Cell* **32**, 169–180.
7. Bussey, H., Saville, D., Greene, D., Tipper, D. J. & Bostian, K. A. (1983) *Mol. Cell. Biol.* **3**, 1362–1370.
8. Bostian, K. A., Burn, V. E., Jayachandran, S. & Tipper, D. J. (1983) *Nucleic Acids Res.* **11**, 1077–1097.
9. Thiele, D. J., Wang, R. W. & Leibowitz, M. J. (1982) *Nucleic Acids Res.* **10**, 1661–1678.
10. Perlman, D. & Halvorson, H. O. (1983) *J. Mol. Biol.* **167**, 391–409.
11. Rogers, D. T., Lemire, J. M. & Bostian, K. A. (1982) *Proc. Natl. Acad. Sci. USA* **79**, 2157–2161.
12. Thill, G. P., Kramer, R. A., Turner, K. J. & Bostian, K. A. (1983) *Mol. Cell. Biol.* **3**, 570–579.
13. Bostian, K. A., Lemire, J. & Halvorson, H. O. (1983) *Mol. Cell. Biol.* **3**, 839–853.
14. Woods, D. R. & Bevan, E. A. (1968) *J. Gen. Microbiol.* **51**, 115–126.
15. Grunstein, M. & Hogness, D. (1975) *Proc. Natl. Acad. Sci. USA* **72**, 3961–3966.
16. Lolle, S., Skipper, N., Bussey, H. & Thomas, D. Y. (1984) *EMBO J.* **3**, 1383–1387.
17. Julius, D., Schekman, R. & Thorner, J. (1984) *Cell* **36**, 309–318.
18. Kurjan, J. & Herskowitz, I. (1982) *Cell* **30**, 933–943.
19. Leibowitz, M. J. & Wickner, R. B. (1976) *Proc. Natl. Acad. Sci. USA* **73**, 2061–2065.
20. Julius, D., Brake, A., Blair, L., Kunisawa, R. & Thorner, J. (1984) *Cell* **37**, 1075–1089.